Journal of Pharmaceutical and Biomedical Analysis 51 (2010) 866–874

Contents lists available at ScienceDirect

Journal of Pharmaceutical and Biomedical Analysis

journal homepage: www.elsevier.com/locate/jpba

Quantitative study of solid-state acid–base reactions between polymorphs of flufenamic acid and magnesium oxide using X-ray powder diffraction

Xiaoming Chen [1], Joseph G. Stowell [2], Kenneth R. Morris [3], Stephen R. Byrn *

Department of Industrial and Physical Pharmacy, School of Pharmacy and Pharmacal Sciences, Purdue University, 575 Stadium Mall Drive, West Lafayette, IN 47907, United States

ARTICLE INFO

Article history:
Received 14 June 2009
Received in revised form
15 September 2009
Accepted 17 September 2009
Available online 14 October 2009

Keywords:
Solid-state
Acid–base reaction
Flufenamic acid
Polymorph
Interactive mix
X-ray powder diffraction

ABSTRACT

The purpose of this study is to investigate solid-state acid–base reactions between polymorphs of flufenamic acid (FFA) and magnesium oxide (MgO) using X-ray powder diffraction (XRPD). Polymorphs of FFA were blended with MgO and stored under conditions of 96.5% RH and 89% RH at 40 °C. The disappearance of FFA and production of magnesium flufenamate were monitored by XRPD. It was observed that the reactions between FFA and MgO proceeded following the Jander equation. Form I of FFA is more reactive with MgO than Form III. Differential accessibility of reactive groups is hypothesized as one of the reasons that Form I is more reactive than Form III. It was noted that the reaction between FFA and MgO could be mitigated by adding another acidic excipient such as polyacrylic acid to prevent the acid–base reaction with FFA. The effectiveness of polyacrylic acid was impacted by the mixing order of the tertiary mixture. Mixing polyacrylic acid and MgO first provided the most significant protection. In conclusion, solid-state acid–base reactions could be investigated using XRPD. Different forms may have distinct reactivity. Acid–base reactions in the solid state could be mitigated through the addition of another "shielding" excipient.

1. Introduction

A solid-state acid–base reaction of an ionized drug with excipients may result in undesirable physical and chemical changes in a solid dosage form. Acid–base reactions involve a change of ionization state of drug molecules and results in a conversion from free form to salt form or vice versa. Because the free and salt forms have distinct physical and chemical attributes, a conversion owing to an acid–base reaction may cause undesired changes in dissolution, bioavailability, appearance, and chemical stability of the solid dosage form. It was reported in the literature that ibuprofen can interact with basic excipients, such as aluminum oxide and kaolin, in the solid state to form an amorphous salt after milling [1,2]. The acid–base reaction triggered the physical transformation of ibuprofen and caused a change in the dissolution rate. A premature acid–base reaction in effervescent tablets has been found to be the main reason for product failure [3]. Despite the potential negative impact of solid-state acid–base reactions on drug quality and stability, there are few literature reports of analytical methodology and reaction kinetics. It is clear that studying this type of reaction in a model system will be beneficial for establishing analytical techniques to detect solid-state changes and instituting formulation strategies to mitigate such an undesirable solid-state interaction.

The stability of solid dosage forms is mainly assayed and quantified by extraction followed by chromatography. However, chromatography is not suitable for testing solid-state acid–base reactions because it can be very difficult to distinguish ionized species from unionized ones in solution. Proton transfer reactions occur much faster in solution than in the solid state so solvent extraction is not acceptable. In addition, information on differential reactivity of solid forms is lost once the material is in solution. It is suggested that solid-state characterization techniques, such as Fourier transform infrared spectroscopy (FT-IR), Raman spectroscopy, X-ray powder diffraction (XRPD), and solid-state NMR, could play a significant role in studying solid-state acid–base reactions. It was demonstrated that FT-IR was very useful in monitoring the interaction of ibuprofen with aluminum oxide and kaolin [1,2]. FT-IR data showed a gradual disappearance of the acid carbonyl peak and a corresponding increase in absorbance of a new signal at 1682 cm^{-1} for the carboxylate in milled ibuprofen powder containing aluminum oxide and kaolin. In another study, FT-IR was applied as a quantitative tool to research the reaction between indomethacin and sodium bicarbonate [4]. In this study, it is

* Corresponding author. Tel.: +1 765 494 1460; fax: +1 765 494 6545.
E-mail address: sbyrn@pharmacy.purdue.edu (S.R. Byrn).
[1] Present address: OSI Pharmaceuticals, Inc., 140 East Hanover Avenue, Cedar Knolls, NJ 07927, United States.
[2] Present address: The Chao Center, 3070 Kent Avenue, West Lafayette, IN 47907, United States.
[3] Present address: Department of Pharmaceutical Sciences, College of Pharmacy, University of Hawaii at Hilo, 34 Rainbow Drive, Hilo, HI 96720, United States.

0731-7085/$ – see front matter © 2009 Elsevier B.V. All rights reserved.
doi:10.1016/j.jpba.2009.09.021

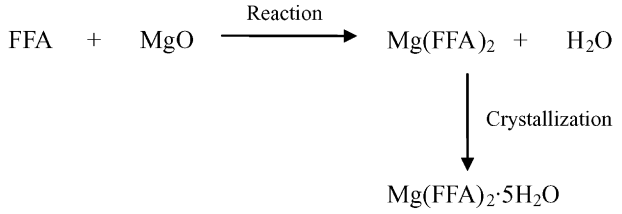

Scheme 1. Solid-state acid–base reaction between flufenamic acid (FFA) and magnesium oxide (MgO).

demonstrated that XRPD can be another powerful tool to monitor solid-state acid–base reaction if one of the reactants or the product is a crystalline material.

XRPD is one of the core techniques used to characterize pharmaceutical solids including drugs and excipients [5]. A pharmaceutical solid in a crystalline form has a unique powder diffraction pattern dictated by its crystal structure, which is a "fingerprint" of the specific crystalline form. XRPD can identify different crystal forms including polymorphs, salt forms, solvates, and hydrates in bulk powders [5,6]. XRPD is also an important quantitative means to determine polymorph and amorphous content, monitor polymorph conversion, follow crystallization of amorphous material, and track hydrate formation and dehydration [7–12]. Acid–base reactions are associated with the disappearance of parent phases and the possible appearance of new crystalline materials. The process is analogous to phase transformations in the solid state. Using flufenamic acid (FFA) as a model compound in this study, it is shown that XRPD can be a very useful tool to detect and monitor solid-state acid–base reactions qualitatively and quantitatively. To our knowledge, this is the first case in the literature to quantify such a type of reaction in a systemic way using XRPD.

FFA is a potent anti-inflammatory agent with analgesic properties for the treatment of rheumatoid arthritis and osteoarthritis [13,14]. The chemical name of FFA is 2-[[3-(trifluoromethyl)phenyl]amino]benzoic acid. It was reported that seven polymorphs exist for FFA [13]. Form I (m.p. 134 °C) is the stable form above 42 °C, while Form III (m.p. 126.5 °C) is the stable form below 42 °C. Form I and III are enantiotropically related to each other. The crystal structure of Form I and III has been reported in the literature [15,16]. As a carboxylic acid, FFA tends to react with basic excipients such as magnesium oxide. The model reaction between FFA and magnesium oxide was extensively researched using XRPD in this study (Scheme 1).

2. Materials and methods

2.1. Materials

Magnesium oxide, potassium nitrate, potassium sulfate, sodium hydroxide, magnesium nitrate, and flufenamic acid (FFA) were purchased from Aldrich. Form I and Form III of FFA were prepared by controlled crystallization from toluene. Flufenamic acid was dissolved in toluene by heat with three times of supersaturation. The supersaturated solution was stirred by a stir bar and cooled down until crystallization observed. The solids were harvested right way to obtain Form I. The harvested Form I was cured in a 100 °C dry oven for 2–3 h to transform any contaminated Form III to Form I. Form III was prepared by taking advantage of the solution mediated conversion of Form I to Form III in toluene. After recrystallization, the crystals was kept at the mother liquid for 2–3 h to ensure all Form I was converted to Form III before harvesting. Samples of both forms were sieved and sieve fractions from 170 to 230 mesh were collected for the study with MgO.

2.2. Setup of reaction mixtures of FFA and MgO

Form I or Form III of FFA was gently triturated with a specified weight of MgO using an agate mortar and pestle. The prepared mixture was kept at 40 °C over a saturated aqueous solution of potassium nitrate (89% RH) or potassium sulfate (96.5% RH). Samples of the stored mixtures were taken for X-ray powder diffraction analysis at selected time intervals.

2.3. Measurement of specific surface area

Specific surface area of all materials was determined in a Micromeritics 2010 BET Surface Area Analyzer using Krypton as the measuring gas with approximately 1 g of material.

2.4. X-ray powder diffraction

All diffraction patterns were measured on a Siemens D500 equipped with a vertical goniometer using Bragg–Brentano ($\theta/2\theta$) geometry. Copper Kα radiation was generated at a power of 40 kV and 20 mA. A Kevex Psi peltier cooled silicon [Si(Li)] detector was used. About 0.25 g powder sample was filled into an aluminum sample holder and gently pressed down by a glass slide to make the sample surface and holder surface coplanar. For qualitative investigation, a continuous scan was recorded for all samples from 4° to 36° 2θ with step size of 0.04° 2θ and scanning rate of 6° 2θ per minute for qualitative investigation. For quantification, a step scan was used for a specific 2θ range with a step size of 0.02° 2θ and a scanning rate of 0.6° 2θ per minute.

2.5. Microscopy

Microscopic analysis was performed with a Zeiss (Jena, Germany) polarized-light microscope connected to a digital camera. The images were recorded with the video program on a Macintosh computer.

2.6. Molecular simulation

Cerius^2 (Accelrys, California) was used to visualize crystal structures, perform geometric measurements, and carry out calculation of powder patterns and morphologies.

3. Results and discussion

3.1. Preparation and characterization of Form I and Form III of flufenamic acid

Both Forms I and III of flufenamic acid (FFA) were used in this study to test the effect of polymorphic form on reactivity with magnesium oxide (MgO). Preparation of the two forms was carried out by controlled crystallization in toluene. It was observed that Form I, a metastable form at room temperature, was first formed from crystallization. The observation agrees with Ostwald's rule of stages of crystallization [17,18]. According to Ostwald's rule, crystallization from solution often occurs in such a way that thermodynamically unstable phases appear first followed by recrystallization to thermodynamically more stable phases. During preparation, Form I must be harvested quickly. Otherwise, a significant amount of Form III would be produced because Form I tends to be converted in a saturated solution to Form III, the stable form at room temperature. To ensure the high purity of Form I, the harvested Form I was cured in a 100 °C dry oven for 2–3 h to convert residual Form III to Form I, the stable form at that temperature. As mentioned in the introduction part, Form I and Form III is an enantiotropic pair with a transition temperature at 42 °C, with Form III as the stable form below 42 °C.

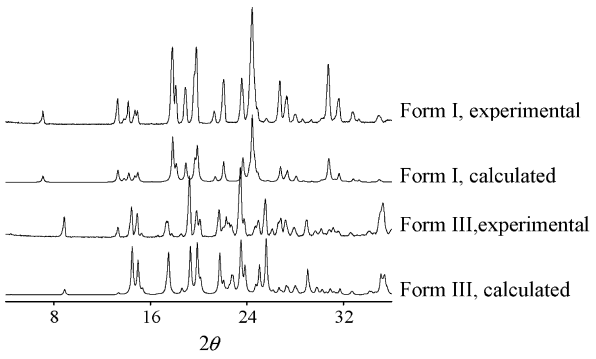

Fig. 1. Comparison of experimental and calculated XRPD of Form I and Form III FFA.

Form III was obtained by stirring the crystals in mother liquid for 2–3 h after crystallization, ensuring that Form I was fully converted to Form III by a solution mediated transformation.

Thermogravimetric (TGA) analysis confirmed that FFA materials obtained from crystallization had less than 0.1% volatile component. The melting point of the prepared two FFA forms from differential scanning calorimetry (DSC) analysis agrees with the literature [13,19]. The experimental diffractograms of prepared Form I and Form III match those calculated from the respective crystal structures, as demonstrated in Fig. 1. Characterization by DSC and XRPD confirmed the nature of Form I and Form III prepared in-house.

The particle size of FFA used for this study was controlled by sieving. The sieve fraction from 170 to 230 mesh was selected to mix with MgO. As shown in Fig. 2, Form I and Form III from 170 to 230 mesh have similar particle size. Form I has a chunk-like morphology, whereas Form III exhibits a thin-plate shape. Owing to morphology difference, the two forms obtained from the same sieve fraction have distinct surface areas. The Form I material has a specific surface area of 0.13 m^2/g, while the Form III material displays a specific surface area of 0.33 m^2/g.

Both Forms I and III of FFA have very good physical stability under the reaction conditions investigated. No physical transformation has been observed for either form at 40 °C, 96.5% RH for up to 2 months. XRPD after storage was found to be identical with the one before storage for both forms.

3.2. Preparation and characterization of magnesium flufenamate

Products of the solid-state acid–base reaction between a FFA polymorph and MgO are expected to be magnesium flufenamate and water. Since magnesium flufenamate is not commercially available, preparation of the magnesium salt was required to characterize and quantify the reaction. FFA was dissolved in an equal molar sodium hydroxide solution to make sodium flufenamate in solution. The sodium flufenamate solution was mixed with magnesium nitrate ($Mg(NO_3)_2$) solution to precipitate out magnesium flufenamate, which is poorly soluble in water. Magnesium flufenamate was collected by filtration and air-dried. XRPD data revealed that the prepared magnesium salt was very crystalline (Fig. 3). Elemental analysis of the dried salt confirmed that the molar ratio between magnesium and flufenamate is 1:2. A 14.5% weight loss was observed in TGA analysis, which suggests that the crystalline salt is a pentahydrate. The deprotonated nature of the salt was also confirmed by proton NMR of the dried material in DMSO and FT-IR of the salt in a KBr pellet.

3.3. Solid-state acid–base reactions of polymorphs of flufenamic acid and magnesium oxide

An acid–base reaction between a FFA polymorph and MgO will result in the disappearance of crystalline flufenamic acid and the

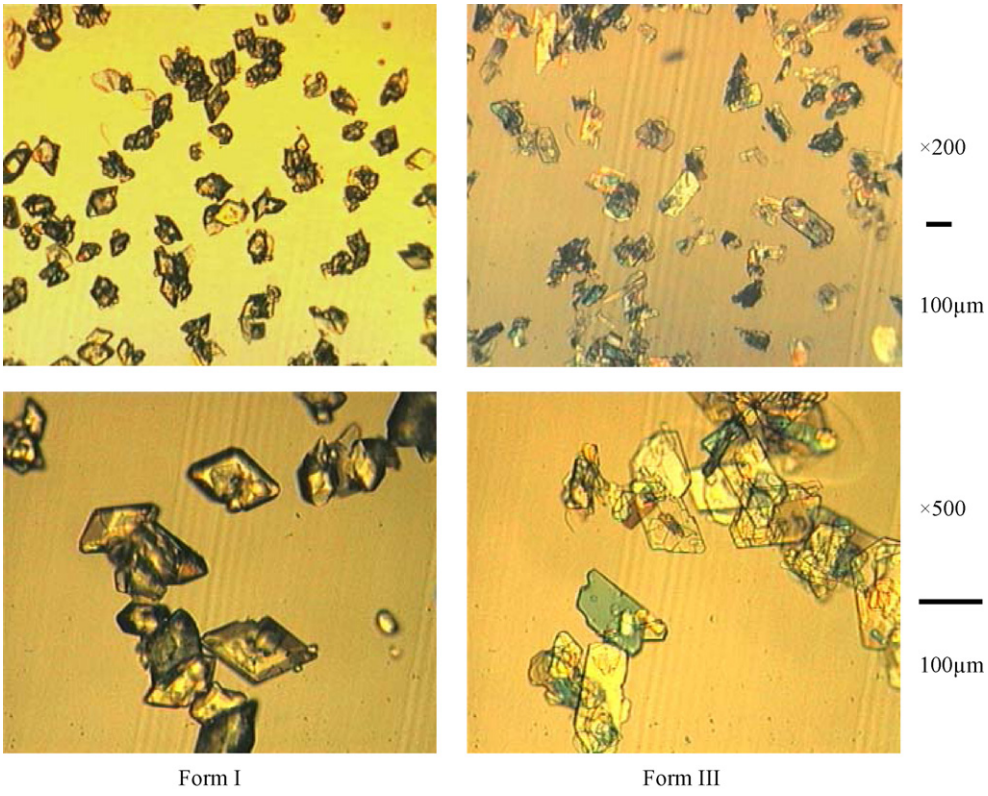

Fig. 2. Microscopic view of Form I and Form III prepared from toluene. Samples were from the 170–230 mesh sieve fraction.

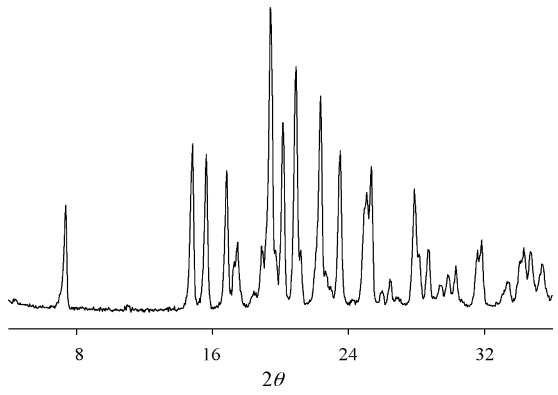

Fig. 3. XRPD of magnesium flufenamate prepared by solution reaction.

production of magnesium flufenamate. Using the method developed in house, those physical changes were detected by XRPD. As shown in Fig. 4, the change in powder pattern of a mixture of FFA Form I and MgO under the storage at 40 °C, 96.5% RH is clearly demonstrated. Form I, from the sieve fraction of 170–230 mesh, was mixed with MgO in a 2:1 molar ratio and stored under 40 °C, 96.5% RH. XRPD revealed that an acid–base reaction occurs between FFA Form I and MgO under the above storage condition. With time, the characteristic diffraction peaks at 13.3°, 13.8°, and 30.8° 2θ of Form I diminished. Simultaneously, diffraction peaks of a new crystalline material formed and increased. Diffractogram peaks of the new material match those of magnesium flufenamate pentahydrate at 7.6°, 15.8°, 16.4° 2θ. These results reveal that Form I of FFA does react with MgO in the solid state to form magnesium flufenamate pentahydrate. A similar transition was observed for the mixture of Form III with MgO under the same storage condition. The same reaction product was produced for both forms. The transition involves chemical and physical changes. The first step is molecular loosening of FFA from its crystal lattice. The second step is its reaction with MgO to form magnesium flufenamate. The last step is the crystallization of magnesium flufenamate pentahydrate. It is

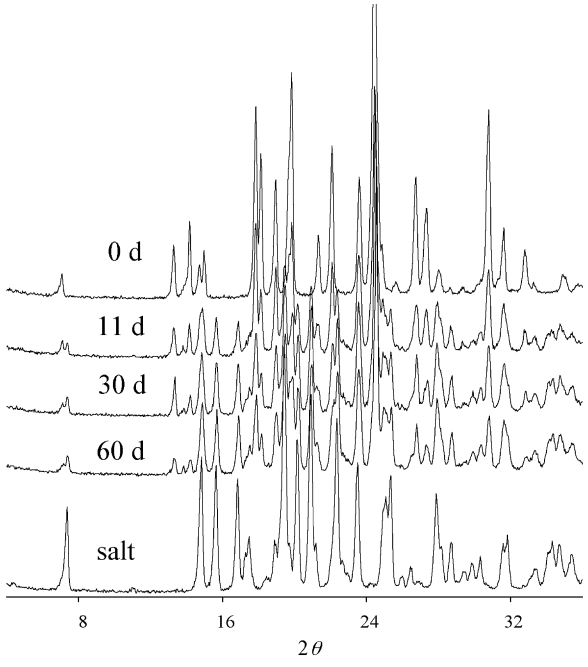

Fig. 4. XRPD of the mixture of Form I of FFA and MgO in 2:1 molar ratio, stored under 40 °C, 96.5% RH for 0, 11, 30, and 60 days. Salt: magnesium flufenamate pentahydrate.

Table 1
Composition of ternary mixtures for creating XRPD calibration curves.

Percentage of reaction	Percentage of FFA	FFA (mg)	MgO (mg)	$Mg(FFA)_2 \cdot 5H_2O$ (mg)
0	93.32	250	17.90	0.00
10	82.88	225	16.11	30.36
20	72.72	200	14.32	60.72
40	53.15	150	10.74	121.46
60	34.56	100	7.16	182.20
80	16.86	50	3.58	242.96
90	8.33	25	1.79	273.30

obvious that the whole transition is a complex process affected by multiple factors, such as temperature, humidity, particle size, and mixing ratio.

3.4. Establishment of a quantitative method based on X-ray powder diffraction

Using unique XRPD peaks of FFA polymorphs and magnesium flufenamate pentahydrate that are well resolved, a quantitative method based on XRPD was developed to monitor the reaction (Fig. 4). To identify a proper calibration method, a series of tertiary mixtures of reactants and product were prepared to reflect the reaction between FFA and MgO mixed in a 2:1 molar ratio (Table 1). XRPD data were collected and analyzed for those standard mixtures. For both forms, several different peaks had been tried for quantification. Only the study of Form I is shown here, since the method development for the two forms is similar.

Representative calibration curves are shown in Fig. 5. The integrated intensity of a specific diffraction peak was plotted against the weight percentage of Form I in the mixture. It was observed that not every well-resolved diffraction peak is suitable for quantification purposes. If a peak is sensitive to preferred orientation,

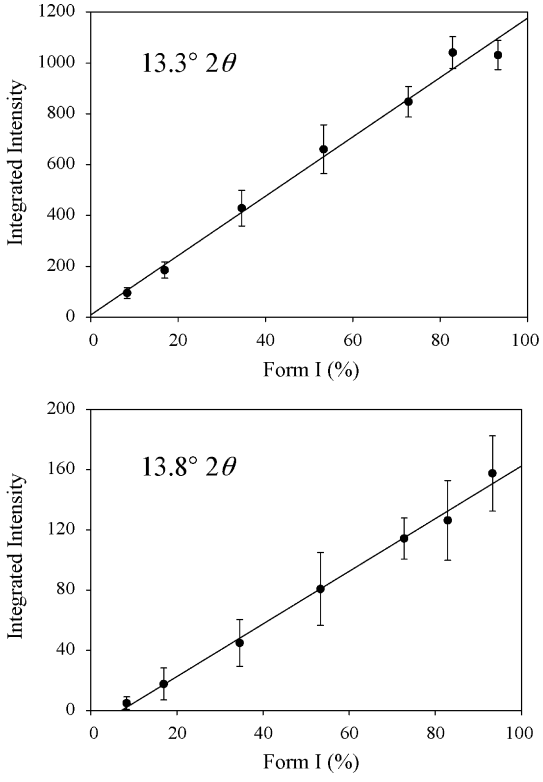

Fig. 5. Representative calibration curves to quantify Form I for its mixture with MgO and magnesium flufenamate pentahydrate ($n = 5$).

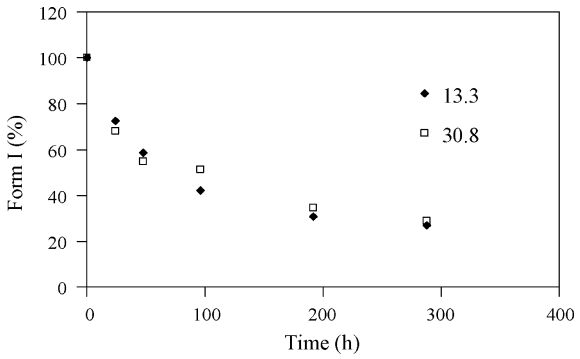

Fig. 6. A reaction between FFA Form I and MgO under the condition of 40 °C, 96.5% RH, quantified by two calibration curves based on peaks at 13.3° and 30.8° 2θ, respectively. The unreacted Form I was monitored.

it is difficult to obtain reproducible data. In the case of the peak at 13.8° 2θ for Form I, the relative standard deviation for each point from five samplings is greater than 15%. In contrast, the calibration curve for the peak at 13.3° 2θ is much better for the same material with a standard deviation of less than 10% for all the data. Among the seven diffraction peaks tested for the 70 μm material, 13.3° and 30.8° 2θ are the best with respect to linearity and precision. Those two peaks were selected to follow the reactions. A quantitative method for Form III in the tertiary mixture was also established. The characteristic peak for Form III at 27.2° 2θ was chosen as the peak for calibration based on linearity, precision, and robustness to preferred orientation.

A calibration curve to quantify the reaction product was also established. The preferred orientation of magnesium flufenamate pentahydrate was much less significant because the average particle size of magnesium flufenamate pentahydrate was about 10 μm. The calibration curve based on the characteristic peak at 15.6° 2θ has near perfect linearity (R^2 = 0.9986) and a very small standard deviation. It confirms the conventional wisdom that XRPD is a very good quantification method if the particle size can be reduced to mitigate the effect of preferred orientation [20]. Particle size and polymorphs of FFA have minimal impact on the calibration curve of magnesium flufenamate pentahydrate. The slopes and intercepts are very similar when magnesium flufenamate pentahydrate was mixed with different particle sizes of either form.

The good linearity of the established calibration curve is consistent with theory [21,22]. The relationship between concentration (C_i) and a specific peak's intensity (I_i) can be simplified, as in the following equation according to Bugay et al. [23]:

$$C_i = B_i \times MAC \times I_i$$

where B_i is the calibration constant and *MAC* is the mass absorption coefficient. *MAC* is dependent on the chemical composition of the mixture. Since, for the reaction between flufenamic acid and MgO, the change in overall chemical composition is minimal, the *MAC* was treated as constant. Thus the relation between concentration and peak intensity is close to linear. The calibration curves established agree with the above assumption.

3.5. Quantification of the reaction between polymorphs of FFA and magnesium oxide using X-ray powder diffraction

With the above calibration methods, reactions between polymorphs of FFA and MgO were investigated quantitatively. As shown in Fig. 6, the quantification data from two different calibration methods gave very good agreement for the reaction between Form I and MgO under 40 °C, 96.5% RH. Those two calibration curves were established from diffraction peaks at 13.3° and 30.8° 2θ, which were less impacted by preferred orientation, as discussed in the previous section.

The generation of product was quantified at the same time. It gave very good mass balance with the disappearance of FFA as shown in Fig. 7. The same good mass balance was also observed for the quantification of reactions with Form III. The mass balance indicates that the acid–base reaction was the only major reaction involved under these conditions. It confirms the validity of the quantification method. It also substantiates that the peaks picked

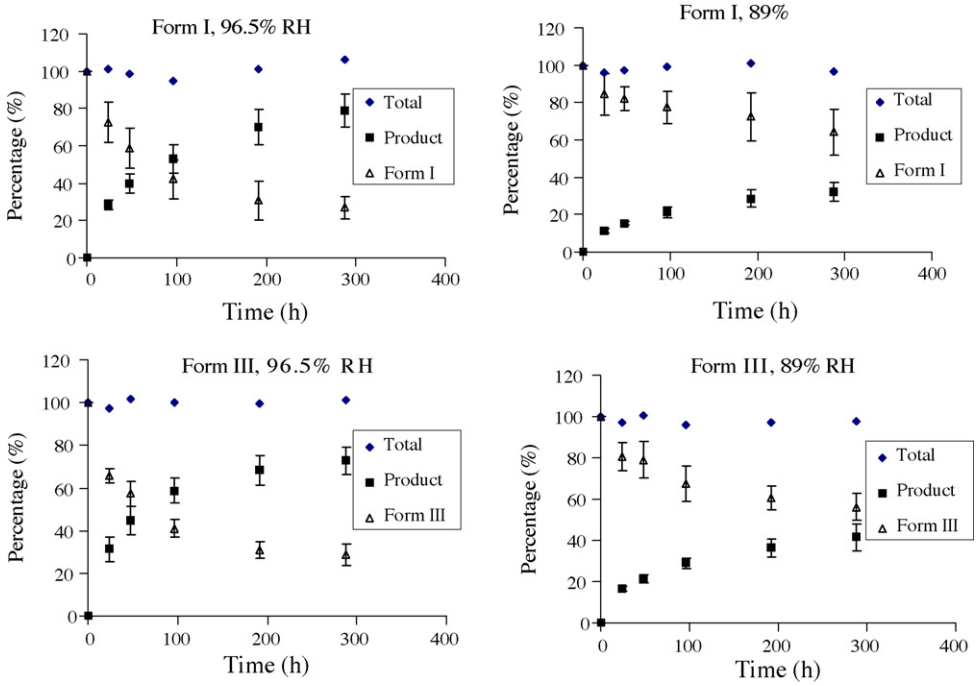

Fig. 7. Mass balance of reactions between polymorphs of FFA and MgO under 40 °C, 96.5% or 89% RH. Form I: unreacted Form I; Form III: unreacted Form III; Product: magnesium flufenamate pentahydrate; Total: the sum of FFA polymorphs and product.

Table 2
Fitting result of the reaction between FFA Form I and magnesium oxide.

Equation	RH = 96.5%		RH = 89%	
	Slope ($\times 10^{-3}$)	R^2	Slope ($\times 10^{-3}$)	R^2
Prout-Tomkins	8.13	0.950	4.71	0.898
Avrami-Erofeev, $n = 1/4$	1.29	0.942	0.73	0.910
Avrami-Erofeev, $n = 1/3$	1.69	0.949	0.86	0.917
Avrami-Erofeev, $n = 1/2$	2.46	0.963	1.02	0.929
Avrami-Erofeev, $n = 2/3$	3.19	0.975	1.07	0.941
Avrami-Erofeev, $n = 1$	4.58	0.991	1.01	0.960
1D phase boundary	1.83	0.938	0.79	0.947
2D phase boundary	1.44	0.970	0.44	0.954
3D phase boundary	1.12	0.978	0.31	0.956
1D diffusion-controlled	2.05	0.982	0.35	0.985
2D diffusion-controlled	1.59	0.994	0.20	0.988
3D diffusion-controlled	0.42	0.997	0.05	0.989
Jander equation	0.58	0.999	0.05	0.991
Power law, $n = 1/4$	0.75	0.882	0.62	0.897
Power law, $n = 1/3$	0.94	0.889	0.73	0.903
Power law, $n = 1/2$	1.27	0.903	0.84	0.916
Power law, $n = 1$	1.85	0.938	0.78	0.947
Zero-order	1.83	0.938	0.79	0.947
First-order	3.55	0.859	3.69	0.876
Second-order	12.63	0.996	1.32	0.972

for quantification reflect the overall disappearance of FFA (for Form I = 13.3° 2θ, for Form III = 27.2° 2θ).

A traditional kinetic study for a solid-state reaction involves the fitting of the kinetic data to different solid-state reaction models. The goodness of fit with one kind of model suggests the reaction follows the associated specific mechanism. The fitting result for the reaction between Form I and MgO in a 2:1 molar ratio is listed in Table 2. The reaction conditions were 40 °C, 96.5% or 40 °C, 89% RH. Models based on diffusion control give a better fit than other models; among them, the Jander equation, a three-dimensional diffusion model, provides the best fit.

Fig. 8 shows the fitting curves of the Jander equation. The fit is excellent and is consistent with the hypothesized mechanism, i.e., that diffusion is controlling. As the acid and base come into contact and form a salt layer, further reaction requires the reactants to diffuse through the product layer. Similar diffusion-controlled kinetics was also observed for the reaction between indomethacin and sodium bicarbonate under 40 °C, 66% RH [4]. For a solid–solid reaction, a layer of the product formed covers the surface of the reactant. The diffusion of reactant through the product layer is much slower than a surface chemical reaction and is the rate-controlling step of the overall reaction. The reaction is de-acceleratory as the product layer becomes thicker. Three-dimensional diffusion control is modeled by Jander equation as described as follows:

$$kt = (1 - (1 - \alpha)^{1/3})^2$$

where α is reacted portion, t is time, and k is a Jander rate constant.

Reaction kinetics with three-dimensional diffusion control have been observed for inorganic systems, such as the reaction between BaO_2 and α-Fe_2O_3 [24], thermal decomposition of plumbo-jarosite [25], and oxidation of FeV_2O_4 [26]. The Jander equation has been applied to interpret the stability data of various pharmaceuticals including the degradation of cyanocobalamin in sugar-coated tablets [27], the instability of propantheline bromide caused by aluminum hydroxide [28], and the crystallization of furosemide solid dispersion in the presence of water vapor [29].

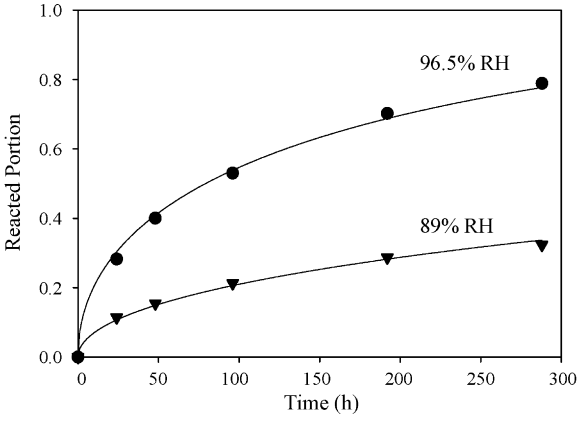

Fig. 8. Fitting curves with the Jander equation for the reactions between FFA Form I (70 μm) and MgO under 96.5% and 89% RH at 40 °C.

3.6. Comparison of FFA Form I and Form III

Solid-state acid–base reactions involve interactions at the surface of the crystals involved. In order to understand the chemical moiety at the crystal surface of FFA polymorphs, the morphology of both Forms I and III was indexed by combining XRPD and optical goniometry. Single crystals of Form I and Form III were prepared by slow evaporation from toluene. Single crystals of Form I and Form III are easily differentiated by color and morphology. Form I is off-white color with a diamond shape. Form III has a light yellow color with a plate-like morphology. For both forms, the major face was characterized by XRPD and indexed by comparing the calculated powder pattern from *Cerius*^{2}. For Form I, the major face was indexed to be (1 0 0); for Form III, (2 0 0) is the major face (space groups $P2_1/c$ and $C2/c$, respectively). The angles between minor faces and the major face were measured with an optical goniometer. A model of the morphology was generated using the morphology platform in *Cerius*^{2}. Starting with a Bravis–Friedel–Donnay–Harker (BFDH) estimate; existing faces of the model were modified to generate a morphology close to the microscopic observation. Indexing for both forms is illustrated in Fig. 9.

As with single crystals, the powder of FFA used for this study was prepared by recrystallization from toluene without seeding. Though Form I is commercially available, recrystallization was still used in order to make the two forms with as similar a sample history as possible since commercial powder is usually subject to milling and has irregular shapes. To obtain the two powders with similar particle size distributions, a sieve fraction of 170–230 mesh was selected for the study with MgO. Microscopic study confirmed that the two forms from this sieve fraction had very similar particle size (Fig. 2). The morphology of both forms was also close to those indexed from single crystals but most importantly, the constituent faces of the morphologies were preserved.

The prepared Forms I and III were mixed with MgO in a 2:1 molar ratio and kept under 40 °C 96.5% RH, and 89% RH. The kinetics data have already been presented in Fig. 7, demonstrating their mass balance agreement. All four groups of data were fit reasonably well with the Jander equation. The obtained rate constants were normalized to the total surface area. At 89% RH, Form I is slightly more reactive than Form III (0.00038 $h^{-1}/(m^2/g)$ vs. 0.00027 $h^{-1}/(m^2/g)$). However, at 96.5% RH, Form I is approximately four times more reactive than Form III (0.0046 $h^{-1}/(m^2/g)$ vs. 0.0012 $h^{-1}/(m^2/g)$). The difference in the reactivity of the two polymorphs is very significant.

In this study, MgO is microcrystalline, with particle size of several microns (29 m^2/g surface area). Those very fine MgO particles attach to the relatively much larger surfaces of the flufenamic acid crystals to form an interactive mix. So the contact efficiency with MgO should be determined by the surface area of FFA. Therefore, the comparison based on normalization to the total surface area

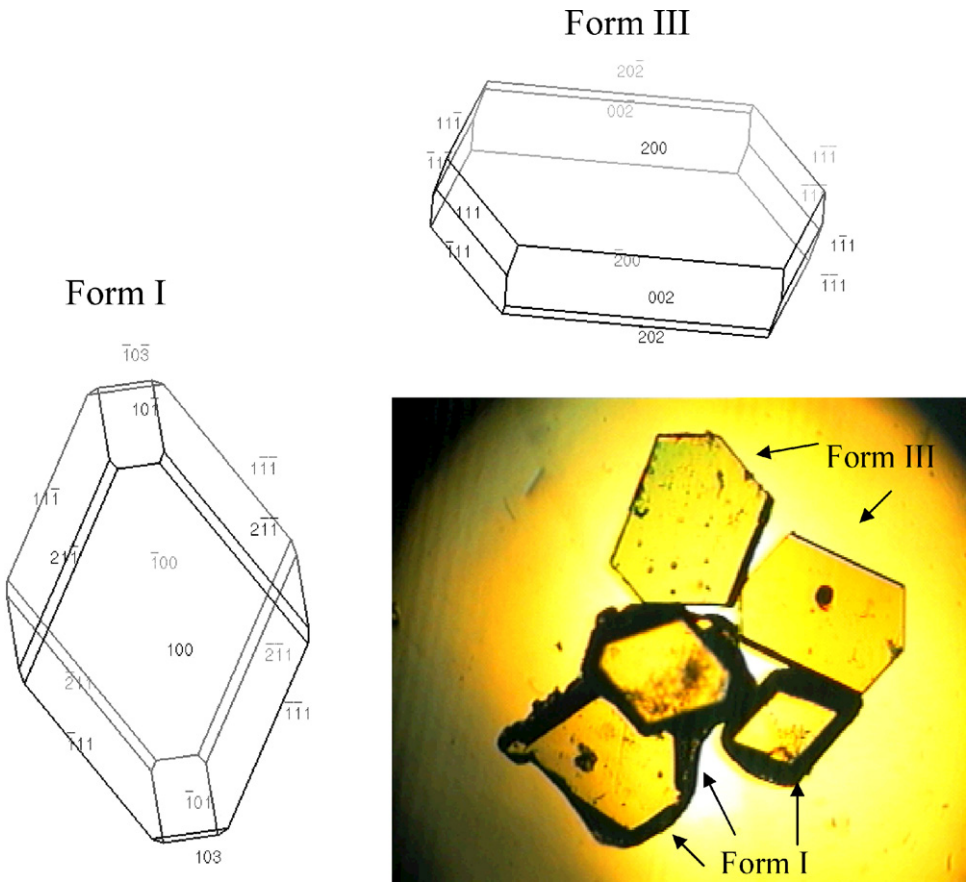

Fig. 9. Comparison of indexed morphology and single crystals of FFA polymorphs prepared from toluene.

of FFA is acceptable to reflect the different reactivity of the two forms.

There are many possible explanations to account for the different reactivity observed. One possibility is that Form I takes up more moisture than Form III via capillary condensation or other mechanisms. However, the moisture sorption experiments showed that both forms gained minimum amounts of moisture after being kept at 40 °C, 96.5% RH for 7 days. The weight gain for Form I was about 0.19% and that for Form III was 0.20%. The moisture uptake behavior cannot, therefore, explain the difference in reactivity for the two forms.

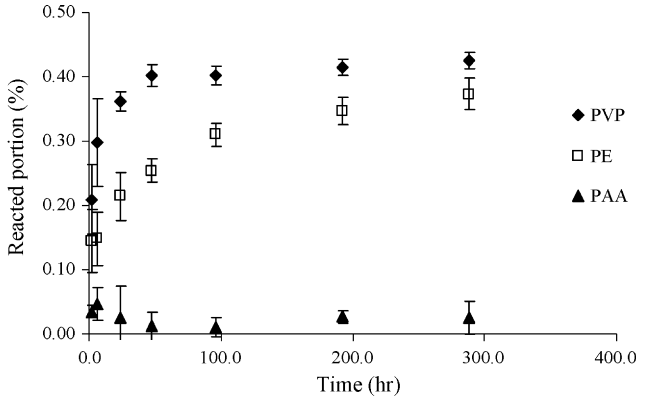

Fig. 10. Reaction kinetics between FFA Form I and MgO in the presence of another excipient such as PE (polyethylene), PVP (polyvinylpovidone), or PAA (polyacrylic acid) under the condition of 40 °C, 89% RH.

Another possibility is that the difference in reactivity is due to dissolution. However, the equilibrium solubility of Form I and Form III in a saturated MgO aqueous solution at 40 °C is nearly equal: Form I has a solubility of 0.473 ± 0.012 mg/mL and Form III has a solubility of 0.451 ± 0.015 mg/mL in saturated MgO aqueous solution. It is likely that they have very similar dissolution rates if there is an aqueous layer present. The solubility data agrees with the thermodynamic relationship between the two forms. It was reported that the transition temperature of the two forms is about 42 °C; the two forms should be very close in free energy at 40 °C. So solubility/dissolution differences do not provide a sound explanation for the different reactivity of the two polymorphs. It was hypothesized that the different reactivity is more related to the reactive group accessibility based on differences in the crystal structure of the two forms.

It was reported that Form I of FFA was more reactive with dry ammonia gas than Form III at room temperature and 60 °C [30]. The reactivity could not be correlated to its thermodynamic stability. It was proposed that the difference in reactivity is due to crystal packing. Form III has more efficient packing than Form I in the major face, which prevents the carboxylic acid group from reaction with ammonia. It is likely that the difference in reactivity of Form I vs. Form III with MgO is also due to the good accessibility of reaction groups of Form I.

3.7. The effect of other excipients on the reaction between polymorphs of FFA and magnesium oxide

Solid dosage forms usually contain multiple components. Other excipients in the formulation may affect the solid-state reaction between an acid and a base.

Table 3
Blend order of the tertiary mixture of FFA Form I, MgO, and PAA.

Blending order	Step 1	Step 2
A	Mixing of Form I and MgO	Add PAA
B	Mixing of Form I and PAA	Add MgO
C	Mixing of PAA and MgO	Add Form I

The effect of common excipients, such as povidone (PVP), polyethylene (PE), and polyacrylic acid (PAA), on the reaction between FFA Form I and MgO were investigated. A tertiary mixture, consisting of 80% of Form I and MgO blend (2:1 molar ratio) with 20% (w/w) of one of the three excipients, was tested. One of the excipients and MgO were blended first before mixing with Form I. The ternary mixtures were kept under 40 °C, 89% RH. The disappearance of Form I was monitored and quantified (Fig. 10). As shown in Fig. 10, the mixture with PVP was the most reactive. The reaction was quickly advanced within 24 h, with 36% Form I reacted. The reaction reached a plateau after the reacted portion reached a 40% loss. The reaction kinetics of the mixture with PE is similar to that of the binary mixture of Form I and MgO kept at the same condition. About 22% Form I was lost within 24 h. The reaction is de-acceleratory with only 38% reacted after 288 h. Compared to PE, PVP facilitates the reaction, which could be due to its well-known ability to take up moisture. The significant uptake of water by PVP greatly catalyzed the reaction between Form I and MgO. However, PAA dramatically inhibits the reaction between Form I and MgO. The acid–base reaction was barely detectable. Only 3% of Form I was lost after 288 h at 40 °C, 89% RH. PAA, as a polymer with carboxylic acid groups, may act as a scavenger for MgO to prevent its further reaction with FFA Form I. It was hypothesized that MgO forms an interactive mixture with PAA, which limits the physical contact of MgO with Form I. The hypothesis is supported by the observation that the inhibitory effect of PAA was dependent on the mixing order of the tertiary mixture.

A tertiary mixture of FFA Form I, MgO, and PAA was blended in different orders as listed in Table 3. The reaction between Form I and MgO at 40 °C and 89% RH was monitored for those three mixtures. It was discovered that the order of mixing affects the degree of reaction between Form I and MgO. Blending sequence A, in which Form I and MgO were mixed first, resulted in the most reaction. The reacted portion is about 20% after 12 days. Blending sequence C, in which PAA and MgO were mixed first, showed the least reaction. Only about 1% of Form I was reacted under storage at the same condition for 12 days. Blending sequence B, in which PAA and Form I were mixed first, had an intermediate reaction, where 8% of Form I was lost. The impact of mixing order on reactivity is very dramatic. The reason is the tendency of MgO to form intimate mixtures with Form I and PAA. MgO used in this study is a microcrystalline material with very fine particle size. When FFA Form I is mixed with MgO first, the interactive mixture is firmly formed. Further mixing with PAA does not reduce the interaction between them. The interactive mixture between Form I and MgO was catalyzed to react by water and temperature. On the other hand, the formation of interactive mixtures of PAA and MgO limits the interaction of MgO with Form I. PAA acts as a scavenger of MgO to inhibit the reaction between FFA Form I and MgO. It indicates that ordered mixing could be another useful approach to mitigate the incompatibility of two components in solid dosage form by reducing the interaction between them.

4. Conclusions

Form I and Form III of flufenamic acid (FFA) can react in the solid state with MgO to form crystalline magnesium flufenamate pentahydrate under 40 °C, 89% and 96.5% RH. It was demonstrated that XRPD is a powerful tool to quantify such a type of reaction. The reaction between FFA and MgO fits the Jander equation and the reaction mechanism is likely to be diffusion-related. Form I is more reactive than Form III, which is related to difference in accessibility of reactive groups. Polyacrylic acid (PAA) can inhibit the reaction between flufenamic acid and MgO. The degree of inhibition depends on the mixing order of the ternary components.

References

[1] S. Mallick, S. Pattnaik, K. Swain, P.K. De, A. Saha, P. Mazumdar, G. Ghoshal, Physicochemical characterization of interaction of ibuprofen by solid-state milling with aluminum hydroxide, Drug Dev. Ind. Pharm. 34 (2008) 726–734.
[2] S. Mallick, S. Pattnaik, K. Swain, P.K. De, A. Saha, P. Mazumdar, G. Ghoshal, A. Mondal, Formation of physically stable amorphous phase of ibuprofen by solid state milling with kaolin, Eur. J. Pharm. Biopharm. 68 (2008) 346–351.
[3] R. Mohrie, Effervescent tablets, in: H.A. Lieberman, L. Lachman, J.B. Schwartz (Eds.), Pharmaceutical Dosage Forms: Tablets, vol. 1, second ed., Informa Healthcare, New York, 1990, pp. 285–328.
[4] X. Chen, U.J. Griesser, R.L. Te, R.R. Pfeiffer, K.R. Morris, J.G. Stowell, S.R. Byrn, Analysis of the acid–base reaction between solid indomethacin and sodium bicarbonate using infrared spectroscopy, X-ray powder diffraction, and solid-state nuclear magnetic resonance spectroscopy, J. Pharm. Biomed. Anal. 38 (2005) 670–677.
[5] S.R. Byrn, R.R. Pfeiffer, J.G. Stowell, Solid State Chemistry of Drugs, second ed., SSCI, Inc., West Lafayette, Indiana, 1999.
[6] G.P. Bettinetti, X-ray diffractometry in the analysis of drugs and pharmaceutical forms, Boll. Chim. Farm. 128 (1989) 149–162.
[7] Z. Német, G.C. Kis, G. Pokol, A. Demeter, Quantitative determination of famotidine polymorphs: X-ray powder diffractometric and Raman spectrometric study, J. Pharm. Biomed. Anal. 49 (2009) 338–346.
[8] N. Chieng, S. Rehder, D. Saville, T. Rades, J. Aaltonen, Quantitative solid-state analysis of three solid forms of ranitidine hydrochloride in ternary mixtures using Raman spectroscopy and X-ray powder diffraction, J. Pharm. Biomed. Anal. 49 (2009) 18–25.
[9] X. Chen, S. Bates, K.R. Morris, Quantifying amorphous content of lactose using parallel beam X-ray powder diffraction and whole pattern fitting, J. Pharm. Biomed. Anal. 26 (2001) 63–72.
[10] I. Fix, K.J. Steffens, Quantifying low amorphous or crystalline amounts of alpha-lactose-monohydrate using X-ray powder diffraction, near-infrared spectroscopy, and differential scanning calorimetry, Drug Dev. Ind. Pharm. 30 (2004) 513–523.
[11] T. Okumura, M. Ishida, K. Takayama, M. Otsuka, Polymorphic transformation of indomethacin under high pressures, J. Pharm. Sci. 95 (2006) 689–700.
[12] D. Zhou, G.G. Zhang, D. Law, D.J. Grant, E.A. Schmitt, Thermodynamics, molecular mobility and crystallization kinetics of amorphous griseofulvin, Mol. Pharm. 5 (2008) 927–936.
[13] J. Krc Jr., Crystallographic properties of flufenamic acid, Microscope 25 (1977) 31–45.
[14] R.J. Flower, Drugs which inhibit prostaglandin biosynthesis, Pharmacol. Rev. 26 (1974) 33–67.
[15] H.M. Krishna Murthy, T.N. Bhat, M. Vijayan, Structure of a new crystal form of 2-{[3-(trifluoromethyl)phenyl]amino}benzoic acid (flufenamic acid), Acta Cryst. B38 (1982) 315.
[16] J.F. McConnell, 3′-Trifluoromethyldiphenylamine-2-carboxylic acid, $C_{14}H_{10}F_3NO_2$ flufenamic acid, Cryst. Struct. Commun. 3 (1973) 459–461.
[17] W.Z. Ostwald, Studien uber die Bildung und Umwandlung fester Korper, Z. Phys. Chem. 22 (1897) 289–330.
[18] J. Nyvlt, The Ostwald rule of stages, Cryst. Res. Technol. 30 (2006) 443–449.
[19] S. Romero, P. Bustamante, B. Escalera, M. Cirri, P. Mura, Characterization of the solid phases of paracetamol and fenamates at equilibrium in saturated solutions, J. Therm. Anal. Calorim. 77 (2004) 541–554.
[20] R. Jenkins, R.W. Gould, D. Gedcke, Quantitative X-ray Spectrometry, second ed., Marcel Dekker, New York, 1995.
[21] L. Alexander, H.P. Klug, Basic aspects of X-ray absorption in quantitative diffraction analysis of powder mixtures, Anal. Chem. 20 (1948) 886–889.
[22] H.P. Klug, L. Alexander, X-ray Diffraction Procedures for Polycrystalline and Amorphous Materials, second ed., Wiley, New York, 1974.
[23] D.E. Bugay, A.W. Newman, W.P. Findlay, Quantitation of cefepime·2HCl dihydrate in cefepime·2HCl monohydrate by diffuse reflectance IR and powder X-ray diffraction techniques, J. Pharm. Biomed. Anal. 15 (1996) 49–61.
[24] K. Watanabe, Kinetics of solid-state reaction of BaO_2 and α-Fe_2O_3, J. Am. Ceram. Soc. 81 (2005) 733–737.
[25] M. Özacar, A. Alp, A.O. Aydin, Kinetics of thermal decomposition of plumbojarosite, J. Therm. Anal. Calorim. 59 (2000) 869–875.

[26] C.P.J. van Vuurena, P.P. Stander, The oxidation kinetics of FeV_2O_4 in the range 200–500 °C, Thermochim. Acta 254 (1995) 227–233.
[27] S. Ohmori, M. Kataoka, H. Koyama, Stability of cyanocobalamin in sugar-coated tablets, Int. J. Pharm. 337 (2007) 161–168.
[28] M. Horioka, T. Aoyama, K. Takata, T. Maeda, K. Shirahama, Degradation of propantheline bromide and dried aluminum hydroxide gel in powdered preparations. Yakuzaigaku 34 (1974) 16–21.
[29] M. Otsuka, M. Onoe, Y. Matsuda, Hygroscopic stability and dissolution properties of spray-dried solid dispersions of furosemide with Eudragit, J. Pharm. Sci. 82 (2006) 32–38.
[30] X. Chen, T. Li, K.R. Morris, S.R. Byrn, Crystal packing and chemical reactivity of two polymorphs of flufenamic acid with ammonia, Mol. Cryst. Liq. Cryst. 381 (2002) 121–131.